

# UCSF

## UC San Francisco Previously Published Works

### Title

Organophosphorus Flame Retardants Inhibit Specific Liver Carboxylesterases and Cause Serum Hypertriglyceridemia

### Permalink

<https://escholarship.org/uc/item/0056z9v2>

### Journal

ACS Chemical Biology, 9(5)

### ISSN

1554-8929

### Authors

Morris, Patrick J  
Medina-Cleghorn, Daniel  
Heslin, Ann  
et al.

### Publication Date

2014-05-16

### DOI

10.1021/cb500014r

Peer reviewed

# Organophosphorus Flame Retardants Inhibit Specific Liver Carboxylesterases and Cause Serum Hypertriglyceridemia

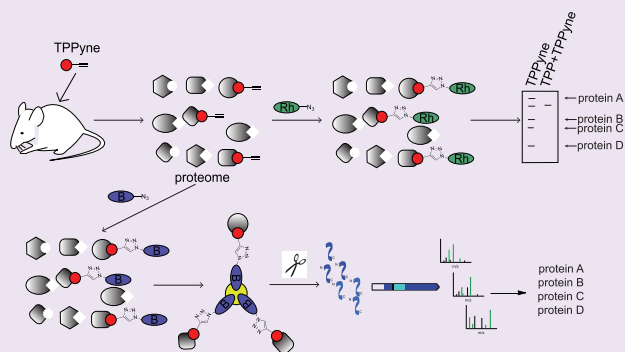
Patrick J. Morris,<sup>§,†</sup> Daniel Medina-Cleghorn,<sup>§,†</sup> Ann Heslin,<sup>†</sup> Sarah M. King,<sup>‡</sup> Joseph Orr,<sup>‡</sup> Melinda M. Mulvihill,<sup>†</sup> Ronald M. Krauss,<sup>‡</sup> and Daniel K. Nomura<sup>\*,†</sup>

<sup>†</sup>Department of Nutritional Sciences and Toxicology, University of California, Berkeley, 127 Morgan Hall, Berkeley, California 94720, United States

<sup>‡</sup>Children's Hospital Oakland Research Institute, 5700 Martin Luther King Jr. Way, Oakland, California 94609, United States

## S Supporting Information

**ABSTRACT:** Humans are prevalently exposed to organophosphorus flame retardants (OPFRs) contained in consumer products and electronics, though their toxicological effects and mechanisms remain poorly understood. We show here that OPFRs inhibit specific liver carboxylesterases (*Ces*) and cause altered hepatic lipid metabolism. Ablation of the OPFR target *Ces1g* has been previously linked to dyslipidemia in mice. Consistent with OPFR inhibition of *Ces1g*, we also observe OPFR-induced serum hypertriglyceridemia in mice. Our findings suggest novel toxicities that may arise from OPFR exposure and highlight the utility of chemoproteomic and metabolomic platforms in the toxicological characterization of environmental chemicals.



Flame retardant chemicals are added to furniture, textiles, vehicle upholstery, electronics, computers, plastics, building materials, hydraulic fluids, and lubricants to prevent combustion and to delay the spread of fires after ignition.<sup>1</sup> Due to their prevalent and increasing utilization in household items and consumer and baby products, human exposure, even at young ages, to flame retardant chemicals is widespread.<sup>1</sup> Organophosphorus flame retardants (OPFRs) are considered to be suitable replacements for legacy brominated flame retardants that have been recently banned or phased out due to toxicity, persistence, and bioaccumulation. OPFR production and application has thus been increasing in recent years. OPFRs have been detected in indoor air, house dust, drinking water, sediment, and biota. More importantly, OPFRs and their metabolites have been detected in 96% of human urine samples.<sup>1,2</sup>

While OPFRs are not acutely toxic in mammals, exposures to these chemicals have been associated with altered hormone levels and reduced semen quality in men.<sup>3</sup> However, other potential long-term health effects are less well understood. Among the OPFRs, triphenyl phosphate (TPP) is one of the most widely used and is considered to be the most effective flame retardant for many polymers (Figure 1a) with staggering levels of use of up to 54 million pounds annually in the United States and Europe. TPP and other OPFRs are major components of Firemaster 550, a flame retardant mixture commonly used in furniture foam at concentrations greater than the legacy flame retardants it replaced.<sup>1</sup> Understanding whether these chemicals interact with biological targets *in vivo*

in mammals to elicit potential toxicological action is thus critical for assessing their long-term adverse health effects.

Here, we utilized integrated chemoproteomic and metabolomic platforms to discover that TPP inhibits several specific carboxylesterase (*Ces*) enzymes *in vivo* in mouse liver, alters hepatic lipid metabolism, and causes serum hypertriglyceridemia. We also present evidence that several additional members of the OPFR chemical class may also inhibit the same set of *Ces* enzymes that cause these dyslipidemic phenotypes.

To identify direct protein targets of TPP *in vivo* in mice, we developed two bioorthogonal chemoproteomic probes that mimic the TPP structure, TPPyne1 and TPPyne2 (Figure 1A). These probes are TPP analogs that include a bioorthogonal alkyne handle that can be reacted with an analytical tag, such as rhodamine-azide or biotin-azide, by copper-catalyzed click chemistry<sup>4,5</sup> for subsequent fluorescent detection or mass spectrometry-based proteomic identification of probe targets, respectively (Figure 1B). We pretreated mice with vehicle or TPP (for 1 h) prior to administration of mice with the TPPyne probes (for 3 h). A rhodamine analytical handle was then appended to the TPPyne-bound proteins in liver lysates *ex vivo* by click chemistry to visualize probe-bound targets. Interestingly, we found that both probes labeled several TPP-specific protein targets *in vivo* in mouse livers, that is, proteins whose

Received: January 8, 2014

Accepted: March 5, 2014

Published: March 5, 2014

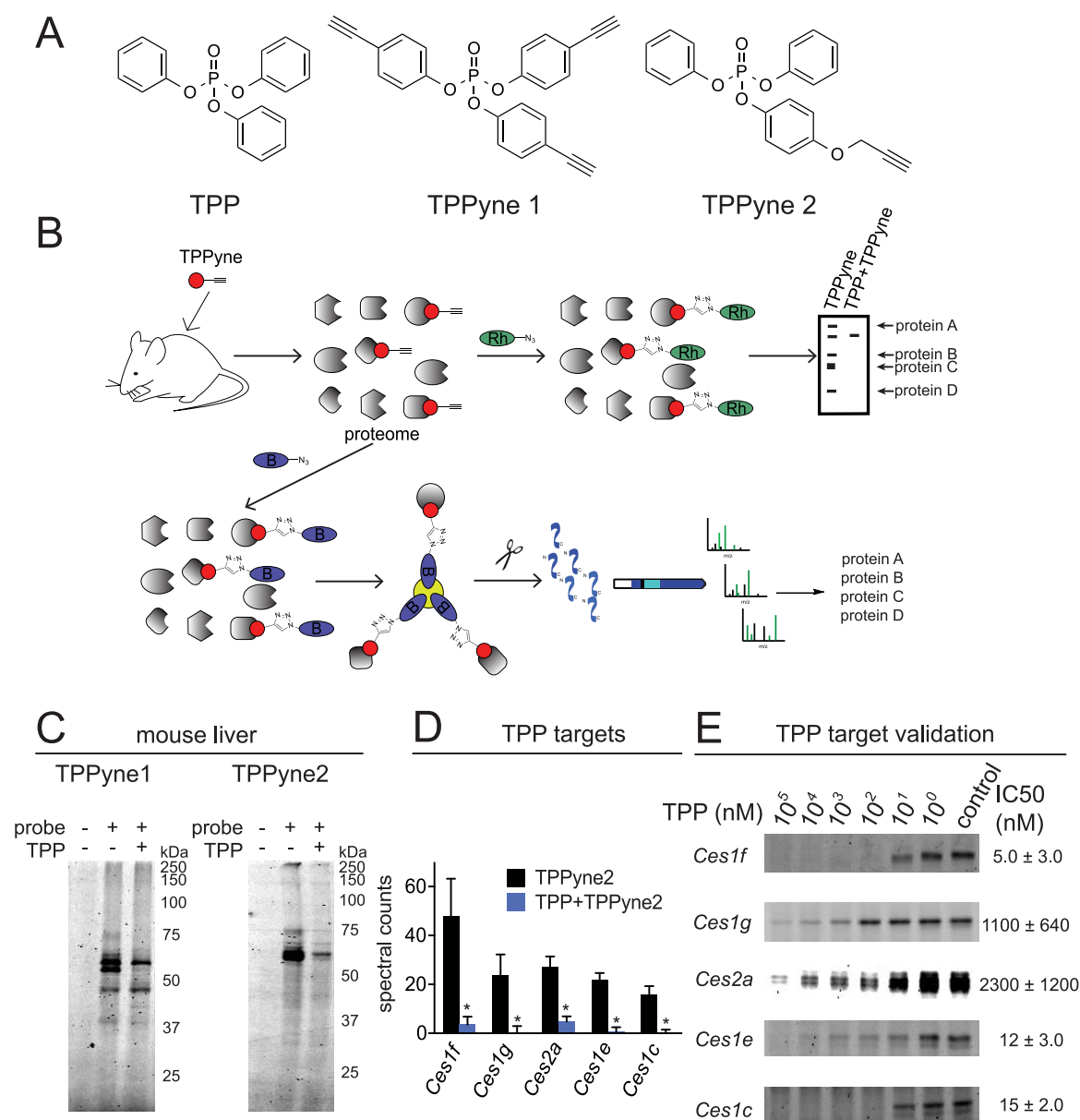


**Figure 1.** Chemoproteomic platforms reveal TPP inhibition of *Ces* enzymes *in vivo* in mouse liver. (A) Structures of TPP and TPP probes TPPyne1 and TPPyne2. (B) Chemoproteomics workflow for C and D: Mice were pretreated with vehicle or TPP (200 mg/kg ip) 1 h prior to treatment with TPPyne1 or TPPyne2 (100 mg/kg, ip) for 3 h *in vivo*. Livers were removed and liver lysates were subjected to click chemistry with (1) rhodamine-azide for SDS/PAGE gel-based fluorescent detection (C) or (2) biotin-azide for avidin-enrichment, tryptic digestion, and proteomic analysis by Multidimensional protein Identification Technology (MudPIT) (D) of probe-bound protein targets. TPP-specific targets were discerned by competition of TPPyne-bound protein targets with TPP by fluorescence or mass spectrometry signal. (C) Gel-based detection of TPPyne1 and TPPyne2 targets in mouse liver. (D) Proteins from TPPyne2-treated mouse livers that were significantly enriched compared to that of TPP-pretreated TPPyne2-treated mouse livers, analyzed by MudPIT and quantified by spectral counting. *Ces1f*, *Ces1g*, *Ces2a*, *Ces1e*, and *Ces1c* are enzymes specifically bound by TPP. (E) Inhibitory potency of TPP against the activities of recombinantly expressed *Ces* enzymes in HEK293T cells as assessed by activity-based protein profiling with the serine hydrolase activity-based probe FP-rhodamine. Inhibitors were pretreated *in vitro* for 30 min at 37 °C prior to incubation with FP-rhodamine for 30 min at 25 °C. Reactions were subsequently terminated and separated on SDS/PAGE and analyzed by in-gel fluorescence. Percent inhibition was determined using Image J and IC<sub>50</sub> values were calculated. Gels in C are representative images of  $n = 3-5$  mice/group. Bar graphs in D and IC<sub>50</sub> values in E are represented as mean ± SEM;  $n = 3-5$  mice/per group in D and  $n = 3$ /group for E. Significance is expressed in D as \* $p < 0.05$  compared with TPPyne2-treated mouse livers.

labeling by the TPPyne probes were competed out by TPP preadministration. TPPyne2 showed more TPP-specific and fewer probe-specific targets compared to TPPyne1, that is, TPPyne1 showed more nonspecific targets that were not competed by TPP, compared to TPPyne2 (Figure 1C). Thus,

we proceeded to use TPPyne2 for subsequent proteomic identification of TPP-specific targets.

To identify the *in vivo* biological targets of TPP, we appended a biotin analytical handle onto proteins labeled by TPPyne2 in liver lysates from the TPPyne2-treated mice using click chemistry, avidin-enriched the probe-labeled proteins,

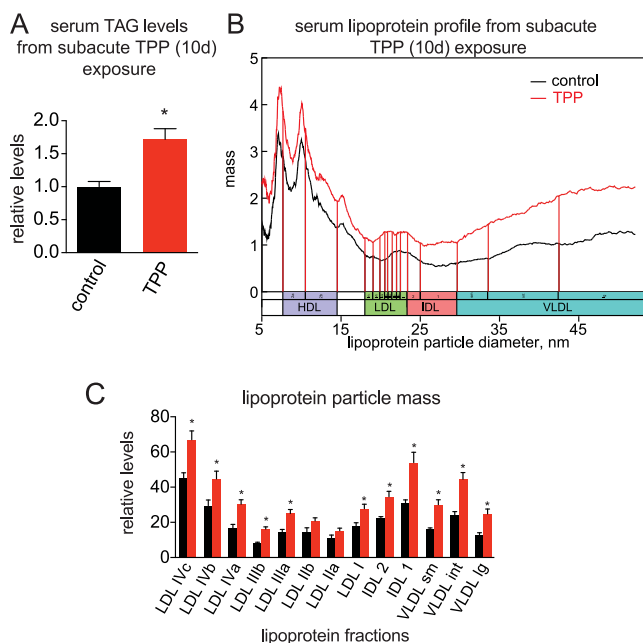


**Figure 2.** TPP induces hypertriglyceridemia and dysregulated lipoprotein profiles. (A–C) Subacute TPP treatment in mice (50 mg/kg, ip, once per day over 10 days) raises serum triacylglycerol (TAG) levels (A), and increased VLDL, IDL, and LDL particle mass (B,C). Lipoprotein profiles and particle mass were determined by ion mobility. Bar graphs in A and C are represented as mean  $\pm$  SEM;  $n = 7$ –10 mice/group (A) and  $n = 3$  mice/group (C). Lipoprotein profiles in B show average values of  $n = 3$  mice/group. Significance is expressed A and C as  $*p < 0.05$  compared with vehicle-treated mice.

trypsinized the enriched proteome, and analyzed subsequent tryptic peptides by Multidimensional Protein Identification Technology (MudPIT).<sup>6</sup> We identified five protein targets from liver lysates that were significantly enriched by the TPPy2 probe ( $p < 0.05$ ) compared with lysates from TPP pretreated TPPy2-treated mice (Figure 1D). We interpret these targets to be TPP-specific protein targets bound *in vivo* in mouse liver. All five protein targets were *Ces* enzymes, *Ces1f*, *Ces1g*, *Ces2a*, *Ces1e*, and *Ces1c*. *Ces* enzymes belong to the serine hydrolase superfamily and have collectively been implicated as both liver triacylglycerol hydrolases and detoxification enzymes for carboxylester xenobiotics.<sup>7,8</sup> In a separate experiment, we tested whether TPP inhibited the activity of these *Ces* enzymes, rather than merely binding these proteins in an activity-independent manner, using activity-based protein profiling (ABPP) coupled to MudPIT (ABPP-MudPIT) with the serine hydrolase activity-based probe, fluorophosphonate-biotin (FP-biotin)<sup>9,10</sup> (Supporting Information Figure S1, Figure S2). ABPP uses active-site directed probes to directly measure the activities of enzymes in complex biological samples.<sup>11–17</sup> Previous studies have shown that the serine hydrolase activity-based probes FP-biotin and FP-rhodamine bind only to active, but not inactive or inhibited, serine hydrolases and can be used to measure the activities of many serine hydrolases, including *Ces* enzymes.<sup>11–17</sup> Indeed, using ABPP-MudPIT, we show that *Ces1f*, *Ces1g*, *Ces2a*, *Ces1e*, and *Ces1c* activities are inhibited by TPP *in vivo*.

We reason that this inhibition of *Ces* activity is through irreversible phosphorylation of TPP to the *Ces* active-site serine, as has been shown for other OP compounds (Supporting Information Figure S3).<sup>13,18</sup> As evidence of this irreversible binding, we show that TPPy2-bound *Ces* targets are visible on a denaturing SDS/PAGE gel and are enriched and identified by proteomics under denaturing conditions (Figure 1C, D). To experimentally determine the nature of this

interaction, we generated a catalytically inactive *Ces1g* Serine 221 to Alanine (S221A) mutant enzyme. We demonstrate that TPPy2 labels wild-type *Ces1g*, but not *Ces1g* S221A, providing evidence of a covalent interaction at the active-site serine of the enzymes, much like other OP compounds that phosphorylate the active-site serine of serine hydrolases to cause functional inhibition (Supporting Information Figure S3). Thus, we propose that TPP likely binds irreversibly to the active-site serine of *Ces* enzymes. Though many OP toxicants have been known to elicit their primary mode of toxicity through acetylcholinesterase (AChE) inhibition, we demonstrate that TPP does not inhibit either acetylcholinesterase (AChE) or butyrylcholinesterase (BChE) activity (Supporting Information Figure S4).

Total carboxylesterase activity has also been previously assayed by measuring *p*-nitrophenyl acetate hydrolysis.<sup>19,20</sup> TPP treatment *in vivo* in mice significantly inhibits total liver *p*-nitrophenyl acetate hydrolytic activity by 43% (Supporting Information Figure S5A). To further confirm that TPP inhibits the activities of the specific TPP target *Ces* enzymes, we next tested whether TPP inhibits *p*-nitrophenyl acetate hydrolytic activity in HEK293T lysates overexpressing the five *Ces* TPP targets. Despite ABPP data showing that all five *Ces* enzymes were overexpressed and active (Figure S5B), *Ces1c* and *Ces1g* did not significantly hydrolyze this substrate (Figure S5C). Only *Ces1e*, *Ces1f*, and *Ces2a* were capable of hydrolyzing *p*-nitrophenyl acetate. Nonetheless, we show that *Ces1e*, *Ces1f*, and *Ces2a* *p*-nitrophenyl acetate hydrolytic activity were completely inhibited by TPP *in vitro* (Figure S5).

We next tested the relative potencies of TPP against the five identified *Ces* enzyme targets recombinantly expressed in HEK293T cells. We found that TPP inhibits *Ces1f*, *Ces1g*, *Ces2a*, *Ces1e*, and *Ces1c* by 50% at concentrations ( $IC_{50}$  values) of 5, 1100, 2300, 12, and 15 nM, respectively (Figure 1E), using competitive ABPP. These  $IC_{50}$  values are within the realm of

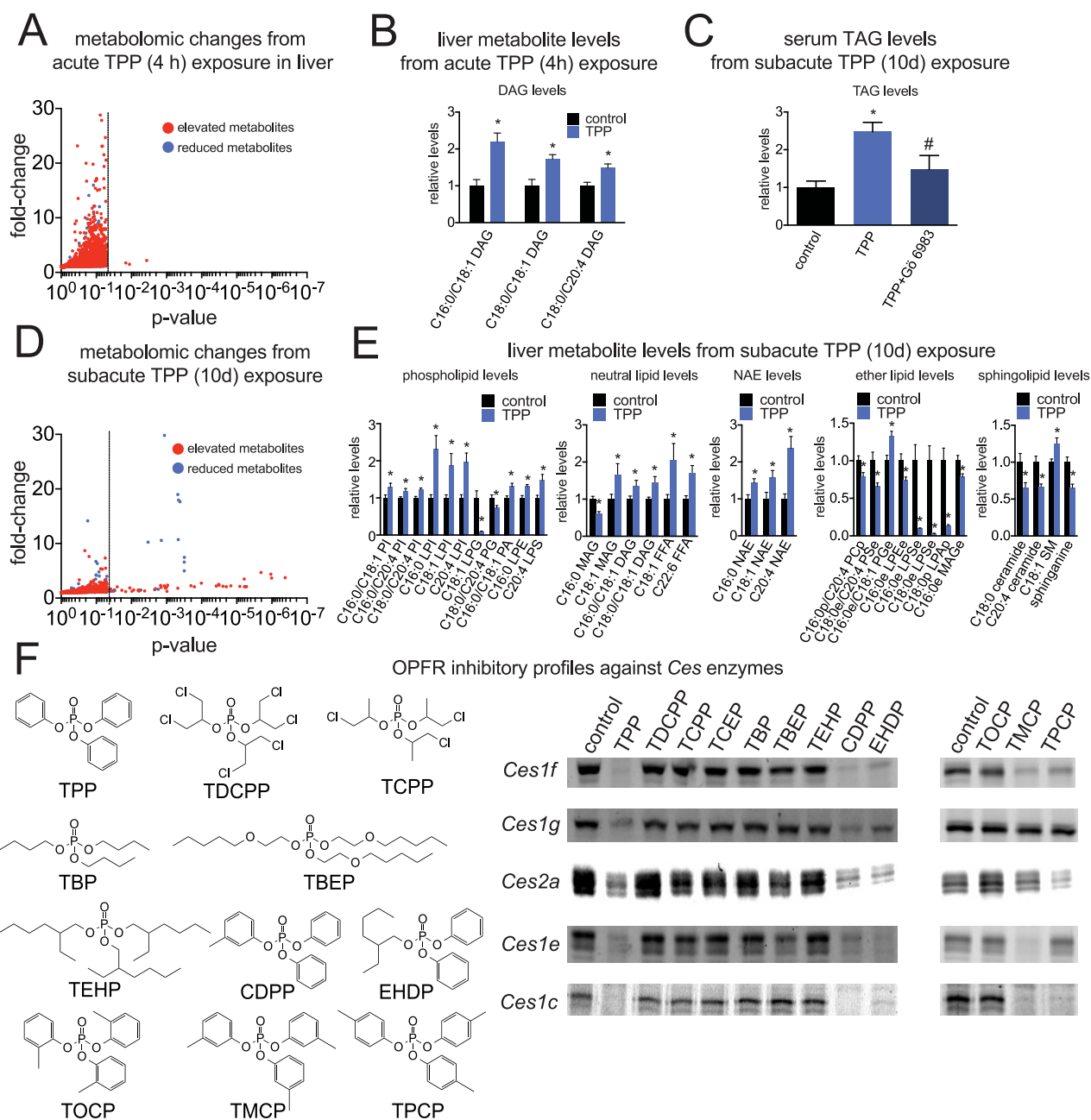


**Figure 3.** TPP causes alterations in hepatic lipid metabolism. (A, B) Metabolomic profiling of livers from mice acutely treated with TPP (100 mg/kg ip, 4 h) in mice. We performed targeted single-reaction monitoring (SRM)-based metabolomics to comparatively profile the levels of ~150 known lipids. We also performed untargeted metabolomic profiling in which we collected all mass spectra between  $m/z$  50–1200 and used XCMSOnline to identify, align, integrate, and compare all detectable ions between control and TPP-treated mice resulting in a comparison of 20 000 ions. Upon identifying metabolites that were significantly and reproducibly altered, we found that acute TPP treatment (A,B) causes elevations in liver diacylglycerol (DAG) levels. (C) Subacute treatments of TPP (50 mg/kg ip) coadministered with pan-PKC inhibitor Gö 6983 (10 mg/kg ip) once per day over 10 days averts the TPP-induced hypertriglyceridemia. (D,E) Subacute TPP treatment (50 mg/kg ip, once per day over 10 days) leads to broader metabolomic changes in liver lipid levels, including increase in phospholipid, neutral lipid, fatty acid, and N-acyl ethanolamine levels as well as decreases in ether lipid and sphingolipid levels. Shown in (A,D) are total ions detected, where data points to the right of the dotted line are ions that were significantly altered, and data points to the left of the dotted line are ions that were detected but not significantly altered. (F) Profiling of other OPFRs against TPP targets *Ces1c*, *Ces1e*, *Ces1f*, *Ces1g*, and *Ces2a* recombinantly overexpressed in HEK293T cells, by gel-based ABPP. Inhibitors (1  $\mu$ M) were preincubated 30 min at 37 °C prior to labeling with FP-rhodamine for 30 min at RT. Gels are representative images. Abbreviations: DAG, diacylglycerol; PI, phosphatidyl inositol; LPI, lysophosphatidylinositol; LPG, lysophosphatidylglycerol; PG, phosphatidylglycerol; PA, phosphatidic acid; LPE, lysophosphatidyl ethanolamine; LPS, lysophosphatidylserine; MAG, monoacylglycerol; FFA, free fatty acid; NAE, N-acyl ethanolamines; PCp, phosphatidylcholine-plasmalogen; PSe, phosphatidylserine-ether; PGe, phosphatidylglycerol-ether; LPSe, lysophosphatidylserine-ether; LPap, lysophosphatidic acid-plasmalogen; MAGe, monoalkylglycerol-ether; SM, sphingomyelin. Data in B and E represented as mean  $\pm$  SEM;  $n = 4$ –5 mice/per group (A, B) and  $n = 7$ –10 mice/group (C, D, E). Significance is expressed in (B, C, E) as \* $p < 0.05$  compared with vehicle-treated mice, #  $p < 0.05$  compared to TPP-treated mice.



potential exposure levels based on the levels of TPP previously detected in house dust.<sup>1</sup>

Previous work by Quiroga et al. revealed that genetic ablation of *Ces1g* (also known as *Ces1* or Esterase-X) in mice caused obesity, hepatic steatosis, and hyperlipidemia.<sup>21</sup> This striking phenotype prompted us to hypothesize that repeated exposure to TPP may result in similar metabolic alterations. Consistent with this premise, subacute exposure to TPP (once per day over 10 days) in mice led to serum hypertriglyceridemia and increased VLDL and LDL masses (Figure 2a–c). Based on findings of Quiroga et al., we conjecture that TPP is eliciting this dyslipidemic phenotype through increased VLDL secretion through hepatic *Ces1g* blockade, as has been previously shown in *Ces1g*-deficient mice.<sup>21</sup> Because the role of *Ces1f*, *Ces2a*, *Ces1e*, and *Ces1c* are unknown in neutral lipid metabolism, it is not clear at present whether the effects of TPP on lipid metabolism are mediated through *Ces1g* inhibition or through any combination of the target *Ces* enzymes. Thus, at this time, based on existing evidence, we attribute the TPP-induced hypertriglyceridemia to *Ces1g* inactivation, and it will be of future interest to determine the individual and combinatorial roles of these five *Ces* enzymes in dyslipidemia. We also show that lipoprotein lipase ( $IC_{50} > 100 \mu M$ ) is not inhibited by TPP (Supporting Information Figure S6), since LPL inhibition may yield similar hypertriglyceridemia phenotypes through impairing uptake of triglycerides from VLDL.<sup>22</sup>

We next wanted to explore the potential mechanism through which TPP causes hypertriglyceridemia. Because *Ces* enzymes are implicated in lipid metabolism, we focused our efforts on profiling the lipidome by performing liquid chromatography/mass spectrometry (LC/MS)-based metabolomic analysis<sup>9,23</sup> to identify biochemical alterations in the livers of TPP-treated mice. We utilized targeted single-reaction monitoring (SRM)-based methods to comparatively profile the levels of >150 lipids in combination with untargeted approaches to broadly profile >20 000 ions between vehicle and TPP-treated mice. Upon acute *in vivo* TPP-treatment, we were surprised to find that the only significant changes in the lipidome were increases in the levels of diacylglycerols (DAGs) (Figure 3A, B; Supporting Information Table S1). While *Ces* enzymes have been implicated in triacylglycerol hydrolysis, our results may indicate that one or all of the *Ces* enzymes inhibited by TPP may regulate liver diacylglycerol metabolism.

We thus hypothesized that the observed increase in serum triglyceride levels may arise from the initial TPP-induced increases in liver DAG levels. As DAGs are endogenous ligands for protein kinase C (PKC)<sup>24</sup> and PKC-deficient mice are protected against dyslipidemia, we postulated that DAG stimulation of PKC in the liver may result in hypertriglyceridemia. Consistent with this premise, subacute coadministration of the pan-PKC inhibitor Gö 6983 with TPP over 10 days averts the TPP-induced serum hypertriglyceridemia (Figure 3C).

Upon subacute (10 day) TPP treatment, we interestingly observed broader changes in the liver lipidome, not only including increases in DAG levels but also increases in the levels of several phospholipids and lysophospholipids, neutral lipids, and fatty acids, and lowering in the levels of several ether lipids and sphingolipids (Figure 3D, E; Supporting Information Table S1). Thus, longer TPP exposure causes widespread alterations in hepatic lipid metabolism.

To examine chemical class-wide effects of other OPFRs currently in use, we tested the inhibitory potential of these

chemicals against the TPP targets identified in this study. While most of the alkylphosphates were inactive against *Ces*, we found that many arylphosphate OPFRs inhibited *Ces1f*, *Ces1g*, *Ces2a*, *Ces1e*, and *Ces1c*, including cresyldiphenylphosphate (CDPP), 2-ethylhexyl diphenylphosphate (EHDP), tri-*meta*-cresylphosphate (TMCP), and tri-*para*-cresylphosphate (TPCP) (Figure 3f). These results suggest that arylphosphate OPFRs may be a chemotype of concern for eliciting dyslipidemic phenotypes through *Ces* inhibition. It will be of future interest to perform similar studies with bioorthogonal mimics of alkylphosphate flame retardant chemicals to identify their potential biological targets *in vivo*. Previous studies have shown that the OP compound bis-nitrophenylphosphate (BNPP) broadly inhibits *Ces* enzyme activity. While we show that BNPP inhibits *Ces1e*, BNPP does not inhibit *Ces1g* activity.<sup>19</sup> Thus, we would not anticipate that exposure to BNPP would elicit dyslipidemic activity (Supporting Information Figure S7).

In conclusion, we show here that TPP inhibits a specific subset of liver *Ces* enzymes. Genetic deletion of one of these *Ces* enzymes, *Ces1g*, has been shown in mice to cause obesity and dyslipidemia. Consistent with TPP inhibition of *Ces1g*, we show that TPP exposure elicits hypertriglyceridemia, and we find that it likely occurs through heightened liver DAG and PKC signaling and further causes alterations in liver lipid metabolism. We also provide evidence that our findings may apply more broadly to the class of arylphosphate OPFRs. Previous studies have shown that TPP inhibits carboxylesterase activity, oftentimes assayed in crude protein mixtures with the nonspecific serine hydrolase substrates. However, there are at least 20 different carboxylesterases in mice and several hundred other serine hydrolases. While these carboxylesterases are highly homologous to each other,<sup>7</sup> recent studies have shown that there may be unique physiological functions for each carboxylesterase. For example, while *Ces1g*-deficient mice exhibit obesity, hepatic steatosis, and dyslipidemia, pharmacological or genetic ablation of *Ces3* show improved glycemia and serum lipid profiles.<sup>12,25,26</sup> We show here that TPP and other arylphosphate flame retardants inhibit particular *Ces* enzymes (*Ces1f*, *Ces1g*, *Ces2a*, *Ces1e*, and *Ces1c*) and show that prolonged TPP exposure results in similar phenotypes observed in *Ces1g*-deficient mice. Thus, in this study, we provide granularity in the specific *Ces* isoforms that are inhibited by TPP and other OPFRs in mouse liver.

Patisaul et al. recently published a provocative study showing gestational and lactational exposure of rats to Firemaster 550, which contains TPP, a mixture of isopropylated triphenylphosphate isomers, 2-ethylhexyl-2,3,4,5-tetrabromobenzoate (TBB), and bis(2-ethylhexyl)-2,3,4,5-tetrabromophthalate (TBPH), caused hallmarks associated with metabolic syndrome, including increased serum thyroxine, advanced female puberty, weight gain, male cardiac hypertrophy, and altered exploratory behaviors.<sup>27</sup> The authors concluded that these effects were likely due to TBB and TBPH acting as endocrine disruptors, and further showed that overall hepatic *Ces* activity, assayed by *p*-nitrophenyl acetate, was inhibited likely due to carboxylesterase metabolism of TBB and TBPH.<sup>27</sup> Our studies suggest instead that the OPFRs in Firemaster 550 likely led to the inhibition in overall *Ces* activity due to the blockade of specific *Ces* enzymes. While we cannot rule out other interactions of TPP with other proteins, or which of the five *Ces* enzymes may be responsible for TPP-mediated phenotypes, we provide compelling evidence that OPFRs may act as dyslipidemic agents through a unique mode of action of

inhibiting *Ces1g* that may be distinct from endocrine disrupting mechanisms. It will be of future interest to develop more selective inhibitors for individual *Ces* enzymes to dissect their individual and combined roles in lipid metabolism. Quite interestingly, while *Ces* activity has been traditionally assayed through measurement of *p*-nitrophenyl acetate hydrolysis, we demonstrate that *Ces1g* does not hydrolyze this substrate, consistent with previous reports<sup>28</sup> and that the observed inhibition of total liver *p*-nitrophenyl acetate hydrolytic activity following TPP exposure is likely due to *Ces1f* inhibition. The inability of *Ces1g* to turnover *p*-nitrophenyl acetate likely reflects a tight binding pocket within *Ces1g* that cannot accommodate di- and triarylphosphonates with substituents on the aryl groups, as reflected by the inability of TMCP and TPCP to inhibit *Ces1g* (Figure 3F). Thus, traditional *Ces* activity assays would not have been able to specifically identify *Ces1g* as a TPP target. Our findings underscore the importance of chemoproteomic platforms in identifying direct targets of chemicals to inform novel toxicological mechanisms.

Previous literature has reported house dust concentrations of TPP up to 1.8 mg TPP/g dust,<sup>1</sup> and an average household contains approximately 1 g of dust.<sup>29</sup> An average small child weighing 12–13 kg carrying ~1 L total blood volume would require absorption of merely 0.33 mg TPP to reach a blood concentration of 1000 nM—a concentration comparable to or greater than the IC<sub>50</sub> values of TPP against the *Ces* enzyme targets identified in this study. Though such an acute exposure may be unlikely, a comprehensive exposure assessment must consider additional factors, including other sources of TPP exposure, the effects of chronic TPP exposure, and any compounding effects of other OPFRs and environmental chemicals that may inhibit *Ces* enzymes. Indeed, a recent study by Meeker et al. examining urinary metabolites of OPFRs suggests direct, stable sources of exposure, and previous studies examining urinary concentrations of TPP metabolites in humans range up to 28.6 μg/L.<sup>30</sup> Furthermore, since these agents are likely acting through irreversible phosphorylation of the *Ces* active site serine nucleophiles, the duration of *Ces* inhibition is dictated by the rate of protein synthesis and turnover, rather than the rate of chemical elimination from the body. Thus, in the current reality of sustained exposure to mixtures of TPP and other OPFRs, even relatively low amounts of TPP may cause a cumulative inhibition of hepatic *Ces* enzymes. There may also be other environmental chemicals that also inhibit *Ces* enzymes. Medina-Cleghorn et al. recently found that chlorpyrifos, a widely used OP insecticide also inhibits many of the liver *Ces* enzymes, as well as other serine hydrolases *in vivo* in mice.<sup>16</sup> It will be of future interest to test whether chronic and low dose TPP exposure will exert dyslipidemia, hepatic steatosis, obesity, and other aspects of the metabolic syndrome.

We also demonstrate the utility of chemoproteomic platforms in identifying the direct biological targets of environmental chemicals, such as OPFRs, to facilitate their toxicological characterization. We also show that metabolomic platforms can be integrated with chemoproteomic strategies to inform potential toxicological mechanisms downstream of chemical–protein interactions. Overall, we put forth that sustained exposure to OPFRs may present a risk to human health by potentially disrupting hepatic lipid metabolism and exerting hypertriglyceridemia through a unique mechanism of inhibiting specific liver *Ces* enzymes.

## METHODS

Methods and any associated references are available in the Supporting Information.

## ASSOCIATED CONTENT

### Supporting Information

Additional figures as described in the text. Methods. This material is available free of charge via the Internet at <http://pubs.acs.org>.

## AUTHOR INFORMATION

### Corresponding Author

\*E-mail: [dnomura@berkeley.edu](mailto:dnomura@berkeley.edu).

### Author Contributions

§P.J.M. and D.M.-C. contributed equally to the work.

### Notes

The authors declare no competing financial interest.

## ACKNOWLEDGMENTS

We thank Dr. Carolyn Bertozzi and Dr. Kathy Collins of the University of California, Berkeley for use of their Typhoon flatbed scanners. This work was supported by the Searle Scholar Foundation, the Center for Environment Research on Toxics, and the National Institutes of Health (P42ES004705).

## REFERENCES

- (1) van der Veen, I., and de Boer, J. (2012) Phosphorus flame retardants: Properties, production, environmental occurrence, toxicity, and analysis. *Chemosphere* 88, 1119–1153.
- (2) Van den Eede, N., Neels, H., Jorens, P. G., and Covaci, A. (2013) Analysis of organophosphate flame retardant diester metabolites in human urine by liquid chromatography electrospray ionisation tandem mass spectrometry. *J. Chromatogr. A* 1303, 48–53.
- (3) Meeker, J. D., and Stapleton, H. M. (2010) House dust concentrations of organophosphate flame retardants in relation to hormone levels and semen quality parameters. *Environ. Health Perspect.* 118, 318–323.
- (4) Tornøe, C. W., Christensen, C., and Meldal, M. (2002) Peptidotriazoles on solid phase: [1,2,3]-Triazoles by regioselective copper(I)-catalyzed 1,3-dipolar cycloadditions of terminal alkynes to azides. *J. Org. Chem.* 67, 3057–3064.
- (5) Rostovtsev, V. V., Green, L. G., Fokin, V. V., and Sharpless, K. B. (2002) A stepwise Huisgen cycloaddition process: Copper(I)-catalyzed regioselective "ligation" of azides and terminal alkynes. *Angew. Chem.* 41, 2596–2599.
- (6) Schirmer, E. C., Yates, J. R., 3rd, and Gerace, L. (2003) MudPIT: A powerful proteomics tool for discovery. *Discovery Med.* 3, 38–39.
- (7) Holmes, R. S., Wright, M. W., Laudederkind, S. J., Cox, L. A., Hosokawa, M., Imai, T., Ishibashi, S., Lehner, R., Miyazaki, M., Perkins, E. J., Potter, P. M., Redinbo, M. R., Robert, J., Satoh, T., Yamashita, T., Yan, B., Yokoi, T., Zechner, R., and Maltais, L. J. (2010) Recommended nomenclature for five mammalian carboxylesterase gene families: Human, mouse, and rat genes and proteins. *Mamm. Genome* 21, 427–441.
- (8) Long, J. Z., and Cravatt, B. F. (2011) The metabolic serine hydrolases and their functions in mammalian physiology and disease. *Chem. Rev.* 111, 6022–6063.
- (9) Medina-Cleghorn, D., and Nomura, D. K. (2013) Chemical approaches to study metabolic networks. *Pflugers Archiv.* 465, 427–440.
- (10) Nomura, D. K., Dix, M. M., and Cravatt, B. F. (2010) Activity-based protein profiling for biochemical pathway discovery in cancer. *Nat. Rev.* 10, 630–638.

- (11) Bachovchin, D. A., and Cravatt, B. F. (2012) The pharmacological landscape and therapeutic potential of serine hydrolases. *Nat. Rev.* 11, 52–68.
- (12) Dominguez, E., Galmozzi, A., Chang, J. W., Hsu, K.-L., Pawlak, J., Li, W., Godio, C., Thomas, J., Partida, D., Niessen, S., O'Brien, P. E., Russell, A. P., Watt, M. J., Nomura, D. K., Cravatt, B. F., and Saez, E. (2014) Integrated phenotypic and activity-based profiling links Ces3 to obesity and diabetes. *Nat. Chem. Biol.* 10, 113–121.
- (13) Evans, M. J., and Cravatt, B. F. (2006) Mechanism-based profiling of enzyme families. *Chem. Rev.* 106, 3279–3301.
- (14) Kidd, D., Liu, Y., and Cravatt, B. F. (2001) Profiling serine hydrolase activities in complex proteomes. *Biochemistry* 40, 4005–4015.
- (15) Liu, Y., Patricelli, M. P., and Cravatt, B. F. (1999) Activity-based protein profiling: The serine hydrolases. *Proc. Natl. Acad. Sci. U.S.A.* 96, 14694–14699.
- (16) Medina-Cleghorn, D., Heslin, A., Morris, P. J., Mulvihill, M. M., and Nomura, D. K. (2014) Multidimensional profiling platforms reveal metabolic dysregulation caused by organophosphorus pesticides. *ACS Chem. Biol.* 9, 423–432.
- (17) Nomura, D. K., and Casida, J. E. (2011) Activity-based protein profiling of organophosphorus and thiocarbamate pesticides reveals multiple serine hydrolase targets in mouse brain. *J. Agric. Food Chem.* 59, 2808–2815.
- (18) Kovarik, Z., Radic, Z., Berman, H. A., Simeon-Rudolf, V., Reiner, E., and Taylor, P. (2004) Mutant cholinesterases possessing enhanced capacity for reactivation of their phosphonylated conjugates. *Biochemistry* 43, 3222–3229.
- (19) Wang, J., Williams, E. T., Bourgea, J., Wong, Y. N., and Patten, C. J. (2011) Characterization of recombinant human carboxylesterases: Fluorescein diacetate as a probe substrate for human carboxylesterase 2. *Drug Metab. Dispos.* 39, 1329–1333.
- (20) Imai, T. (2006) Human carboxylesterase isozymes: Catalytic properties and rational drug design. *Drug Metab. Pharmacokinet.* 21, 173–185.
- (21) Quiroga, A. D., Li, L., Trötzmüller, M., Nelson, R., Proctor, S. D., Köfeler, H., and Lehner, R. (2012) Deficiency of carboxylesterase 1/esterase-x results in obesity, hepatic steatosis, and hyperlipidemia. *Hepatology* 56, 2188–2198.
- (22) Wang, H., and Eckel, R. H. (2009) Lipoprotein lipase: From gene to obesity. *Am. J. Physiol.: Endocrinol. Metab.* 297, E271–288.
- (23) Benjamin, D. I., Cozzo, A., Ji, X., Roberts, L. S., Louie, S. M., Mulvihill, M. M., Luo, K., and Nomura, D. K. (2013) Ether lipid generating enzyme AGPS alters the balance of structural and signaling lipids to fuel cancer pathogenicity. *Proc. Natl. Acad. Sci. U.S.A.* 110, 14912–14917.
- (24) Jornayvaz, F. R., and Shulman, G. I. (2012) Diacylglycerol activation of protein kinase Cepsilon and hepatic insulin resistance. *Cell Metab.* 15, 574–584.
- (25) Lian, J. H., Quiroga, A. D., Li, L., and Lehner, R. (2012) Ces3/TGH deficiency improves dyslipidemia and reduces atherosclerosis in Ldlr(−/−) mice. *Circ. Res.* 111, 982.
- (26) Dominguez, E., Galmozzi, A., Chang, J. W., Hsu, K.-L., Pawlak, J., Li, W., Godio, C., Thomas, J., Partida, D., Niessen, S., O'Brien, P. E., Russell, A. P., Watt, M. J., Nomura, D. K., Cravatt, B. F., and Saez, E. (2014) Integrated phenotypic and activity-based profiling links Ces3 to obesity and diabetes. *Nat. Chem. Biol.* 10, 113–121.
- (27) Patisaul, H. B., Roberts, S. C., Mabrey, N., McCaffrey, K. A., Gear, R. B., Braun, J., Belcher, S. M., and Stapleton, H. M. (2013) Accumulation and endocrine disrupting effects of the flame retardant mixture Firemaster 550 in rats: An exploratory assessment. *J. Biochem. Mol. Toxic.* 27, 124–136.
- (28) Ko, K. W., Erickson, B., and Lehner, R. (1991) Es-x/Ces1 prevents triacylglycerol accumulation in McArdle-RH7777 hepatocytes. *Biochim. Biophys. Acta* 1133–1143, 2009.
- (29) Elliott, L., Arbes, S. J., Harvey, E. S., Lee, R. C., Salo, P. M., Cohn, R. D., London, S. J., and Zeldin, D. C. (2007) Dust weight and asthma prevalence in the National Survey of Lead and Allergens in Housing (NSLAH). *Environ. Health Perspect.* 115, 215–220.
- (30) Reemtsma, T., Lingott, J., and Roegler, S. (2011) Determination of 14 monoalkyl phosphates, dialkyl phosphates and dialkyl thiophosphates by LC-MS/MS in human urinary samples. *Sci. Total Environ.* 409, 1990–1993.